



CHORUS

This is the accepted manuscript made available via CHORUS. The article has been published as:

Effect of particle size on the glass transition

Ryan J. Larsen and Charles F. Zukoski

Phys. Rev. E **83**, 051504 — Published 13 May 2011

DOI: [10.1103/PhysRevE.83.051504](https://doi.org/10.1103/PhysRevE.83.051504)

The effect of particle size on the glass transition

Ryan J. Larsen and Charles F. Zukoski

Department of Chemical and Biomolecular Engineering, University of Illinois at Urbana-Champaign, 114 Roger Adams Laboratory, 600 South Mathews Avenue, Urbana, Illinois 61801.

The glass transition temperature of a broad class of molecules is shown to depend on molecular size. This dependency results from the size dependence of the pair potential. A generalized equation of state is used to estimate how the volume fraction at the glass transition depends on the size of the molecule, for rigid molecule glass-formers. The model shows that at a given pressure and temperature there is a size-induced glass transition: for molecules larger than a critical size, the volume fraction required to support the effective pressure due to particle attractions is above that which characterizes the glassy state. This observation establishes the boundary between nanoparticles, which exist in liquid form only as a dispersion in low molecular weight solvents, and large molecules which form liquids that have viscosities below those characterized by the glassy state.

I. INTRODUCTION

The glass transition has been observed in both molecular and colloidal systems.[1-3] A common feature of these systems is that they are granular in nature: they comprise discrete particles that are thermal.[4] Generally speaking, particle diameters in systems of small molecules are less than 1 nm, whereas colloidal systems consist of particles in the range of nanometers to microns. Particles that are close to 1 nm in diameter are intermediate between colloidal and molecular systems but encompass particles of technological significance, including molecular gelators, globular proteins, and nanoparticles.[5-8] Particles in this size range exhibit features that are intermediate between colloidal and molecular systems. They can be dispersed in a solvent, thereby resembling a colloidal phase. However, they can also provide plasticizing effects that are usually associated with small molecules.[9] Because these systems are intermediate between colloidal and molecular, an understanding of their properties requires concepts from both fields of study.

Colloidal particles in a dispersion are commonly characterized by a pair potential of mean force that is mediated by the solvent. Perhaps the simplest pair potential that can be achieved experimentally is the hard sphere potential, in which the particles exhibit an infinite repulsion at contact. The hard sphere potential has been used extensively to model both colloidal and molecular systems.[3,4] Hard sphere systems are known to exhibit a dramatic slow-down in particle dynamics, or glass transition, near a volume fraction, ϕ , of 0.58.[3,10,11] This value is generally taken to be independent of the particle diameter, σ . [12] The size-independence underscores the geometrical nature of the glass transition in hard spheres. It also implies that, to

the extent that both colloidal and molecular systems resemble hard spheres, generic features of the glass transition may be consistent as the particle size continuously transitions from molecular to colloidal length scales.

In general, particles of greater size exhibit greater van der Waals attractions and are more likely to form dense, or glassy, phases with long relaxation times under standard temperature and pressure (STP).[13,14] As a result, in the limit that particles approach the colloidal size regime, they will not form a liquid at STP unless a solvent is introduced. The solvent reduces the effective attractions between particles, thereby dispersing them into solution and forming a colloidal dispersion.[13,15] These observations imply that in the continuum of particle sizes, there exists a boundary that can be used to distinguish between molecular and colloidal systems: particles that are less than the critical size can form single component liquids, whereas particles greater than the critical size require an additional component, or solvent, to form fluid phases, and are therefore colloidal. Here we define the critical size to be the largest size for which a material can exhibit liquid-like behavior, which is the glass transition. Of particular interest is an approach to the glass transition at constant pressure and temperature, in which the size of molecules, or particles, is continuously increased.

The purpose of this paper is to characterize this transition for rigid, non-polar particles, and to elucidate the mechanisms by which larger particles give rise to denser phases. We first use literature data to empirically establish how the strength of attraction depends on molecular size for non-polar molecules in the size range of 0.3 to 0.9 nm. This allows us to develop an equation of state for a generalized van der Waals molecule that depends only on the size of the molecule and which enables us to predict the volume fraction at atmospheric pressure as a function of temperature for any given particle size. We then compare these predictions to experimental data obtained from a variety of rigid nonpolar globular molecules. This comparison allows us to predict how the volume fraction at the glass transition depends on the size of the molecule. We then use the equation of state to study the size-induced approach to the glassy state, showing that at a fixed externally applied pressure, the effective pressure due to molecular attractions changes little during the size-induced increase in density. We use this insight to model the size-induced glass transition with a simplified equation of state in which the effective pressure due to attractions depends only on temperature and not on the size of the molecule. Our approach for analyzing the dependence of phase behavior on molecular size is relevant for understanding the transition from molecular particles to colloidal particles, and limitations of the colloidal description of matter.

II. THEORETICAL

To find a general dependence of the strength of attraction on the size of the molecule we use an equation of state that includes parameters that describe both characteristics: the Carnahan-Starling (CS) equation of state with a van der Waals (vdW) attraction term added to it.[14] The CS-vdW equation of state is

$$Z = \frac{Pv}{k_B T} = \frac{1 + \phi + \phi^2 - \phi^3}{(1 - \phi)^3} - 4 \left(\frac{\tau}{T} \right) \phi \quad (1)$$

where Z is the compressibility, P the pressure, v the volume per molecule, k_B is the Boltzmann constant, T is the temperature, τ parameterizes the strength of attraction, and ϕ is the volume fraction

$$\phi = \frac{\pi \sigma^3}{6v} \quad (2)$$

where σ is the hard sphere diameter. Eq. (1) has been used to predict values for the molecular parameters σ and τ from knowledge of the density at various P and T .^[14] Values of hard sphere volumes, $V_{hs} = \pi \sigma^3 / 6$, calculated using this method are consistent with other measures of molecular volume for a wide variety of molecules.¹⁴ In this approach, a given molecular system is characterized in terms of values of σ_0 and τ_0 at temperature $T_0 = 20$ °C and their derivatives with respect to temperature,

$$\gamma = T \frac{\partial \tau}{\partial T} \quad (3)$$

and

$$\chi = T \frac{\partial \sigma}{\partial T}, \quad (4)$$

evaluated at $T_0 = 20$ °C. From Ref. [14] we extract values of σ_0 , τ_0 , γ , and χ for 20 non polar organic molecules that vary in σ_0 from 0.35 nm to 0.84 nm. In order from smallest to largest these molecules include methane, ethane, propane, butane, ethylene, propene, n-pentane, isopentane, neopentane, n-hexane, cyclohexane, methylcyclohexane, n-octane, isooctane, n-nonane, n-dodecane, n-hexadecane 3,3-diethylpentane, 4,4-dipentylheptane, and 5,5-dibutylnonane. Because these molecules are non-polar, we expect that the interactions between these molecules are dominated by van der Waals forces and therefore represent a set of molecules experiencing minimal attractions. We use this set of molecules to establish how material parameters depend, on average, on the size σ_0 of the molecule.

A plot of τ_0 as a function of σ_0 for all 20 molecules reveals that to a surprising extent, τ_0 is a linear function of σ_0 (see FIG. 1). From a linear fit to the data,

$$\tau_0 = B_1 \sigma_0 + B_2 \quad (5)$$

we obtain $B_1 = 6909 \text{ K/nm}$ and $B_2 = -2021 \text{ K}$.

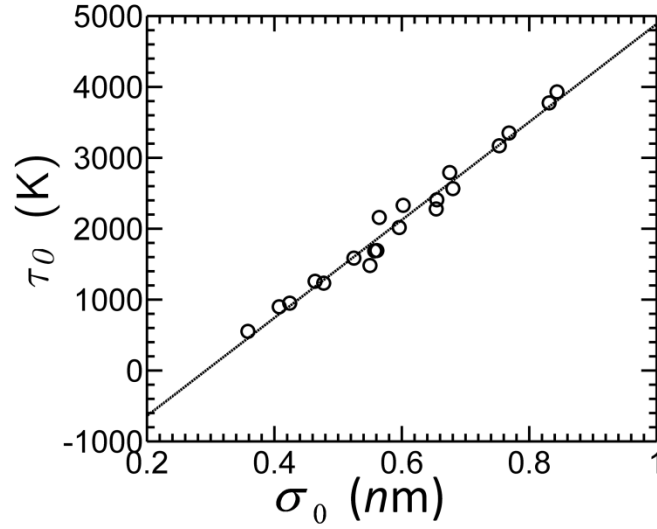


FIG. 1 The dependence of the molecular attraction, τ_0 , on the molecular size, σ_0 for 20 organic nonpolar molecules at 20 °C and atmospheric pressure. The dashed line shows the linear fit, as described in the text. Data from Ref. [14].

We also find that values of γ become more negative as σ_0 increases, suggesting that the temperature sensitivity of the attraction increases with σ_0 , as shown in FIG. 2. We fit this dependence using

$$\gamma = C_1\sigma_0 + C_2, \quad (6)$$

where $C_1 = -3036 \text{ K/nm}$ and $C_2 = 1142 \text{ K}$.

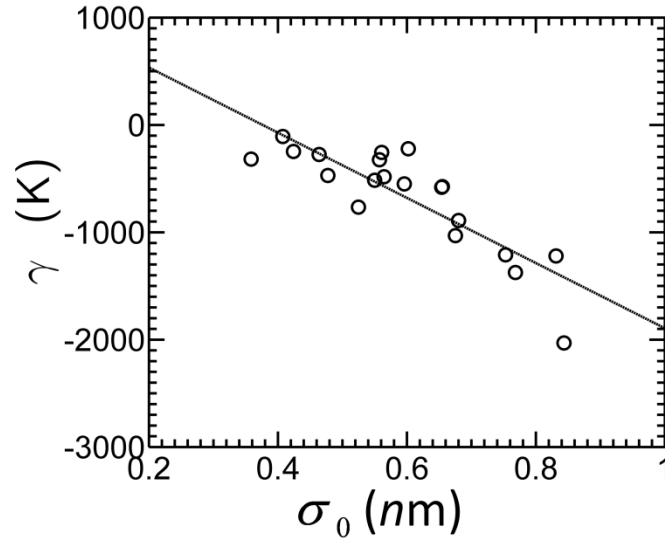


FIG. 2 The dependence of γ on the molecular size, σ_0 for 20 organic nonpolar molecules at 20 °C and atmospheric pressure. The dashed line shows the linear fit, as described in the text. Data from Ref. [14].

Finally, we find that values of χ are roughly independent of σ_0 , as shown in FIG. 3. This indicates that the balance of repulsions and attractions defining the effective hard core diameter is a weak function of T . The average value of χ is $\bar{\chi} = -0.0183$ nm.

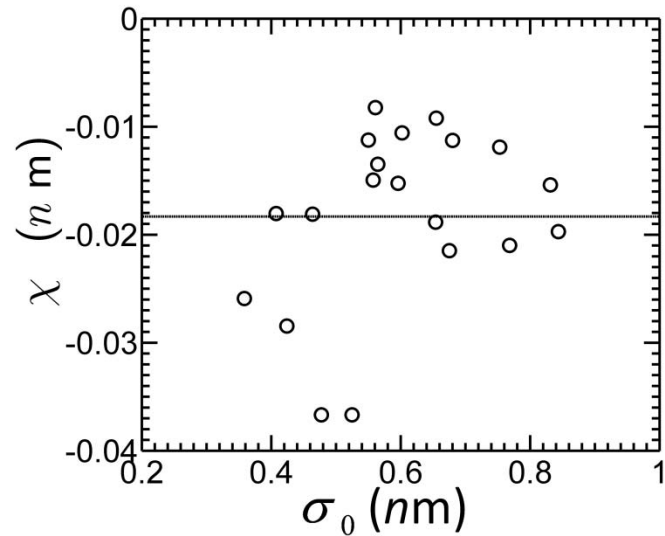


FIG. 3 The dependence of χ on the molecular size, σ_0 for 20 organic nonpolar molecules at 20 °C and atmospheric pressure. The average value, $\bar{\chi} = -0.0183$ nm, is shown by the dashed line. Data from Ref. 14.

Using the relations obtained from the fits, it is possible to calculate values of ϕ for a given combination of σ_0 , T , and P . For a given value of σ_0 this is done by first using the coefficients B_i , C_i , and $\bar{\chi}$ to calculate values of τ_0 , γ , and χ respectively. Values of τ and σ at temperature, T , are then calculated using the relations[14,16]

$$\sigma(T) = \sigma^* \left[1 + \frac{\sqrt{T}}{\sqrt{T_\sigma}} \right]^{-1/6} \quad (7)$$

$$\tau(T) = \tau^* \left[1 + \frac{T_\tau}{T} \right] \quad (8)$$

where parameters in the equations are obtained from σ_0 , τ_0 , γ , and χ with the relations

$$\sigma^* = (\sigma_0)^{7/6} [\sigma_0 + 12\chi]^{-1/6} \quad (9)$$

$$\sqrt{T_\sigma} = -\sqrt{T_0} [1 + (\sigma_0 / 12) / \chi] \quad (10)$$

$$\tau^* = \tau_0 + \gamma \quad (11)$$

$$T_\tau = -T_0 [1 + \tau_0 / \gamma]^{-1} \quad (12)$$

where volumes are expressed in units of \AA^3 and temperatures are expressed in units of Kelvin.[14,16]

The result is an equation of state that is written in terms of a single parameter: σ_0 . Although this relation neglects variation between molecules, it provides a generalized, or average relationship as a function of molecular size. These equations are expected to be accurate over a range of pressures and temperatures near atmospheric conditions for materials in the liquid regime. Here we apply the equations in the region near the glass transition, which exceeds the limits of their intended applicability. We expect that this approach is acceptable because the temperature-dependence of the liquid density generally exhibits liquid-like behavior for temperatures greater than T_g . [17] Nevertheless, our results are intended only as a first order estimate intended to capture general trends in the size-dependence of the glass transition.

III. RESULTS

Our objective is to investigate the mechanisms by which the size of the particle determines the transition to a dense and glassy phase. The equation of state allows us to predict ϕ for any combination of σ_0 , T , and P . In hard sphere colloidal systems, the volume fraction at the glass transition, ϕ_g , is generally observed to occur at a critical value that is independent of particle size. This suggests the hypothesis that in molecular systems values of ϕ_g are independent of σ_0 . If this is the case, then from inspection of Eq. (1), we expect that $T_g \propto \sigma_0$. This scaling relation is obtained by assuming that $\tau \propto \sigma_0$, and that at atmospheric pressure, the term $Z = P_V/k_B T \ll 1$ can be neglected. We test this hypothesis by numerically seeking solutions, (σ_0, T) to the generalized equation of state for fixed values of ϕ and, P , chosen here to be atmospheric pressure. As expected, calculated values of T increase with σ_0 in an approximately linear manner, as shown in Fig. 4 for $\phi = 0.62, 0.66, 0.70$, and 0.74 . These lines are slightly non-linear because of the dependence of τ on the temperature, as expressed by Eq. (6). As expected, the lines of lower ϕ correspond to higher temperatures.

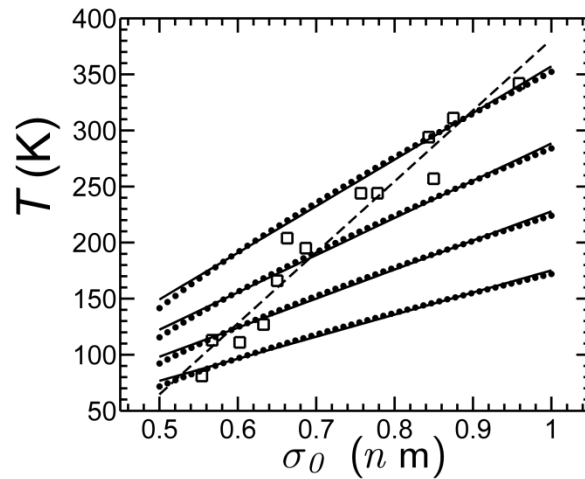


FIG. 4 Values of T_g are predicted using a generalized equation of state by calculating lines of constant volume fraction (shown by the dotted lines). Values of ϕ corresponding to each line are shown to the right of the plot. Linear fits to the lines are shown by solid lines. Experimental values of σ_0 and T_g are shown by the open squares and listed in Table 1. The dashed line is linear fit to the experimental data. Parameters obtained from all linear fits are listed in Table 2.

	σ_0	T_g	Ref.
1. cyclohexene	0.55	81	18
2. toluene	0.57	113	18

3. ethylbenzene	0.60	111	18
4. iso-Propylbenzene	0.63	127	19
5. 4 tert-butyl pyridine (4-TBP)	0.65	166	20
6. phenolphthalein-dimethylether (CGE)	0.66	204	21
7. dimethylphthalate (DMP)	0.69	195	20
8. o-terphenyl	0.76	244	19
9. triepoxide N-N-diglycidyl-4-glycidylloxylaniline (DGGOA)	0.78	244	21
10. phenolphthalein-dimethylether (PDE)	0.84	294	22
11. diglycyl ether of bisphenol A (DEGBA)	0.85	257	21
12. kresolphthalein-dimethylether (KDE)	0.88	311	22
13. 1,3, 5-tri- α -naphthyl benzene	0.96	342	23

Table 1. Values of hard sphere diameter, σ_0 , and T_g for non-polar organic molecules of various size. The right-hand column lists the references from which values of T_g are obtained. The hard sphere diameter is obtained from the hard sphere volume, V_{hs} , which is calculated by first using the molecular increments approach to calculate the van der Waals volume, V_S . Values of V_S are converted to V_{hs} using an empirical relation.[14] The data are plotted in Fig. 4.

If the glass transition were to occur at a critical value, ϕ_g , for all σ_0 , we would expect values of T_g to fall along one of the predicted lines. To test the validity of this hypothesis we have gathered glass transition temperatures of organic molecules of a variety of sizes, listed in Table 2. To ensure that our data set comprises molecules that are approximately rigid,[19] we have not included molecules with alkane chains greater than 3 carbons. We have also chosen molecules that do not have strong polar interactions, and that are therefore expected to interact primarily through van der Waals forces. For each molecule we calculate a van der Waals volume, V_S , by using the molecular increments approach.[24,25] We then convert values of V_S to V_{hs} , by using an empirical relation, $V_{hs} = 1.086(V_S - 9.94)$, [14] where volumes are expressed in \AA^3 . When the experimental values of T_g are plotted as a function of σ_0 , several trends are apparent. First, there

is a general trend to larger values of T_g with increasing σ_0 . Secondly, the experimental glass transition temperatures generally fall between the lines of constant volume fraction predicted by the generalized equation of state for $\phi = 0.62$ and $\phi = 0.74$, as shown in FIG. 4. The slope of the dependence of T_g on σ_0 is greater for the experimental data than the slopes of the lines of constant ϕ predicted by the equation of state (see Table 2). This suggests that the volume fraction, ϕ_g , at the glass transition decreases as the size of the molecules increases. This result is consistent with the expectation that the glass transition is not an iso-free volume point.[26-28]

	A_1 (K/nm)	A_2 (K)
$\phi = 0.62$	415	-59
$\phi = 0.66$	332	-44
$\phi = 0.70$	259	-31
$\phi = 0.74$	196	-21
Experimental	633 ± 44	-252 ± 32

Table 2. Parameters calculated from fits to the equation $T_g = A_1\sigma_0 + A_2$. The first four rows are from fits to values of T_g calculated using the generalized equation of state at various values of ϕ . The final row is from a fit to the experimental data shown in Table 1. Lines from the fits are shown in FIG. 4.

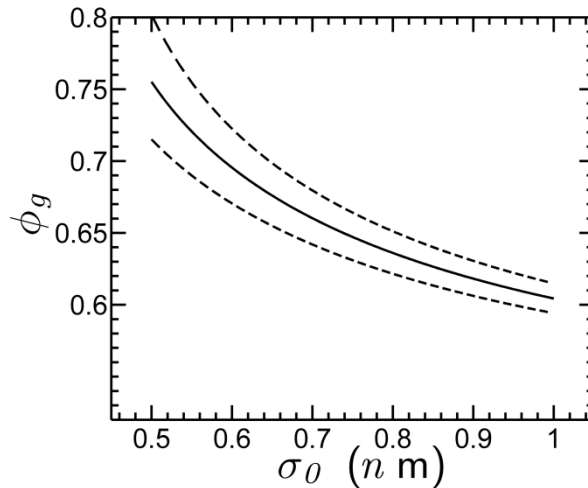


FIG. 5. The linear fit to the experimental data (shown by the dashed line in FIG. 4) is used with the generalized equation of state to estimate values of the volume fraction, ϕ_g , at the glass

transition as a function of σ_0 , shown by the solid line. The dashed lines show the estimated uncertainty in ϕ_g based on the uncertainty in values of A_1 and A_2 obtained from the experimental data and shown in Table 2.

By assuming that the linear fit to the experimental data characterizes $T_g(\sigma_0)$ for the generalized molecule, we are able to calculate ϕ_g for all points along the line $T_g(\sigma_0)$. The resulting function, $\phi_g(\sigma_0)$, increases to higher values as σ_0 decreases, as shown in FIG. 5.

IV. DISCUSSION

The σ_0 -dependence of ϕ_g that is implied by our results suggests that the glass transition in molecular systems differs from that in hard spheres, for which ϕ_g is generally taken to be independent of size. . One possible explanation is that in molecular systems the glass transition is sensitive to the details of the molecules, including shape, anisotropy, and deformability.[29-31] Particles that are slightly non-spherical in shape exhibit values of random close packing that are larger than those associated with spherical particles.[32] As the shape of the particle transitions from spherical to a more anisotropic shape, there is also an increase in the critical ϕ for the dynamical crossover predicted by mode coupling theory.[33] These effects are useful for rationalizing trends that are apparent in our data. The larger molecules, such as o-terphenyl and 1,3,5-tri- α -naphthyl benzene are more spherical than the smaller molecules, many of which contain planar rings. If the non-spherical shape of the smaller molecules allows them to pack more efficiently, they would be expected to exhibit higher values of ϕ at the glass transition than the larger molecules. This trend is indeed consistent with the experimental data.

It is also possible to rationalize our result that ϕ_g decreases with size without invoking differences in the particle shape. Even in the idealized case in which all molecules exhibit an identical shape, the van der Waals approach, in which the attractions are replaced by an effective pressure is not necessarily appropriate for describing the effect of attractions on the dynamical effects associated with the glass transition.[34,35] In one study, the validity of the van der Waals approach was tested by replacing the attractive portions of the Lennard Jones pair potential with a pressure calibrated to enforce an equivalent density.[34] For viscous liquids, the van der Waals approach underestimates the timescales for particle motion by as much as three orders of magnitude.³⁴ However, in the glassy regime, very small changes in volume fraction can produce changes in relaxation time scales of this magnitude. We conclude that the van der Waals approach can be used to provide a first order estimate of ϕ_g : to a first approximation, the van der Waals approach would predict that $\phi_g \approx \phi_{g-vdw}$, which is independent of size. Additional effects that arise from the attractions may be accounted for with higher order corrections to this

estimate. In applying such corrections, we expect that increasing the strength of molecular attractions increase the difference between ϕ_{g-vdw} and the true ϕ_g . Because larger molecules exhibit greater attractions, then $\phi_{g-vdw} - \phi_g$ would be expected to increase with σ . This would tend to cause values of ϕ_g to decrease with increasing σ : particles of greater size would exhibit lower values of ϕ_g because they exhibit greater attractions. This trend is also consistent with our results.

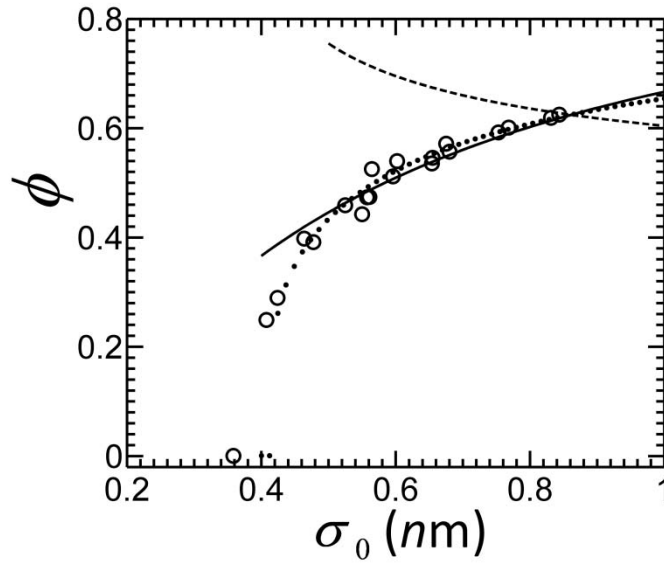


FIG. 6 The dotted line shows the σ -induced increase in ϕ at STP, calculated by using the generalized equation of state. The open circles show values of ϕ calculated directly from values of τ_0 and σ_0 at STP for the 20 molecules used to develop the generalized equation of state. The dashed line shows ϕ_g , as shown in FIG. 5. The difference between the two lines is $\phi - \phi_g$ and controls the proximity to the glass transition. At STP, a σ_0 -induced glass transition occurs when $\phi = \phi_g$, at near 0.9 nm. The solid line is an approximation of the σ -induced increase in ϕ , obtained by setting $P_{eff} = \bar{P}_{eff} = 0.25$ GPa for all σ_0 .

Although the van der Waals approach may not accurately model the effects attractions on dynamics, it can still be used to estimate structure,[34] and is therefore expected to give reasonable estimates of ϕ_g . Knowledge of ϕ_g can provide a geometrical characterization of the proximity to the glass transition. The difference, $\phi - \phi_g$, is linked to dynamical relations through free volume theory. In principle, the glass transition can be approached either by increasing ϕ

or by decreasing ϕ_g . The decrease in ϕ_g with increasing σ_0 suggests the possibility that larger molecules may be more glassy, or solid-like, because ϕ_g , is lower for these particles. We probe the importance of this effect, relative to σ -induced increase in ϕ , by using the generalized equation of state.

We first calculate the σ -induced increase in ϕ at $T = 20$ °C and atmospheric pressure, or STP. The trends in $\phi(\sigma)$ are consistent with values of ϕ calculated for the 20 individual molecules used to obtain Eqs. (5) and (6), as shown in FIG. 6. The generalized equation of state predicts that for $\sigma < \sigma_1 = 0.42$ nm, there is no dense phase and the material is a gas. As σ increases from σ_1 to $\sigma_2 = 1.0$ nm, the volume fraction of the liquid phase increases continuously. In this range of σ there is also a continuous decrease in ϕ_g , as shown by the dashed line in FIG. 6. The σ -dependent increase in ϕ and decrease in ϕ_g both cause the difference $\phi - \phi_g$ to continuously decrease until it vanishes at 0.86 ± 0.03 nm. For larger sizes, the material is a glass. We therefore expect that for hard sphere-like molecules of size greater than approximately 0.9 nm, no liquid state is available. This justifies the use of $\sigma \approx 1$ nm as a natural boundary between molecular and colloidal materials.

This distinction between molecular and colloidal only applies to materials composed of monodisperse particles that are rigid, nonpolar and therefore hard sphere-like. For such materials, the free volume originates only from the thermal energy associated with the hard particles. Alternatively, liquid phases can be obtained by larger particles to which polymeric materials have been grafted.[36] In this case the free volume necessary to form the liquid will originate from the small molecules associated with the polymers and not from the large particles. Likewise, polymer melts or star polymers can also form liquid phases at high molecular weights. However, these resemble chains or networks of hard particles. Modeling the size dependence of systems with significant internal degrees of freedom is beyond the scope of the present work. In this work we focus on systems that resemble unassociated hard particles because these are relevant to the limit in which large and rigid molecules continuously approach the size of hard colloidal particles.

Because the continuous increase in σ drives the system towards a σ -induced glass transition by causing ϕ to increase, we examine in more detail the mechanisms responsible for this effect. It is reasonable to hypothesize that the increase in ϕ with σ occurs because the associated increase in τ causes the effective pressure due to attractions, P_{eff} , to also increase, thereby reducing the system volume. We test this hypothesis by calculating P_{eff} ; the expression for P_{eff} is obtained by rearranging Eq. (1),

$$P = \frac{kT}{v} \left(\frac{1 + \phi + \phi^2 - \phi^3}{(1 - \phi)^3} \right) - \frac{2\pi k_B \tau \sigma^3}{3v^2} = P_{HS} - P_{eff}. \quad (13)$$

During the σ -induced increase in ϕ at STP, calculated values of P_{eff} do not continuously increase with σ , but exhibit a maximum at $\sigma_M = 0.65$ nm, as shown in FIG. 7. This represents an apparent contradiction; as the size of the molecule is increases for $\sigma > \sigma_M = 0.65$ nm, the liquid becomes more dense, even though P_{eff} decreases.

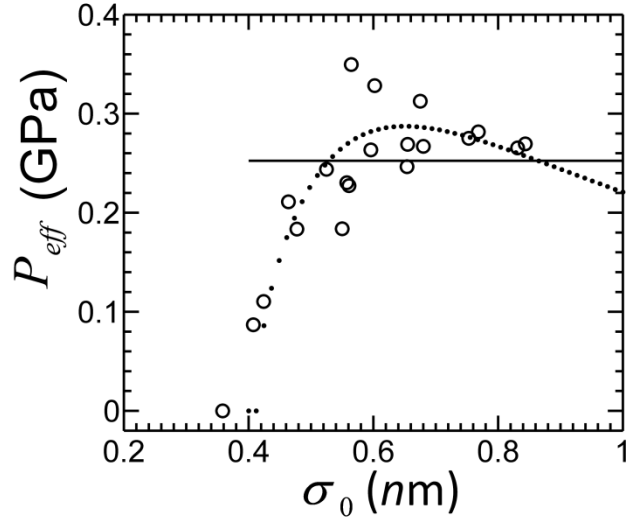


FIG. 7 The dotted line shows the change in P_{eff} during the σ -induced increase in ϕ at STP, calculated using the generalized equation of state. The open circles show values of P_{eff} calculated directly from values of τ_0 and σ_0 for the 20 molecules used to obtain the generalized equation of state. The solid line shows $\bar{P}_{eff} = 0.25$ GPa, calculated by averaging values of P_{eff} over the range of $\sigma_1 = 0.42$ nm to $\sigma_2 = 1.0$ nm.

We justify this observation with a further rearrangement of Eq. (13),

$$\left(\frac{\pi \sigma^3}{6k_B T} \right) P_{eff} \approx \left(\frac{\pi \sigma^3}{6k_B T} \right) (P_{eff} + P) = \phi \left(\frac{1 + \phi + \phi^2 - \phi^3}{(1 - \phi)^3} \right) \quad (14)$$

and note that the expression on the right hand side of the equation increases monotonically with ϕ . From this we observe that an increase in ϕ can coincide with a decrease in P_{eff} if there is a sufficiently large decrease in the entropic stress, $k_B T / \sigma^3$. Because the entropic stress drives particle spreading, a decrease in the entropic stress favors higher values of ϕ , as illustrated in the schematic diagram shown in FIG. 8.

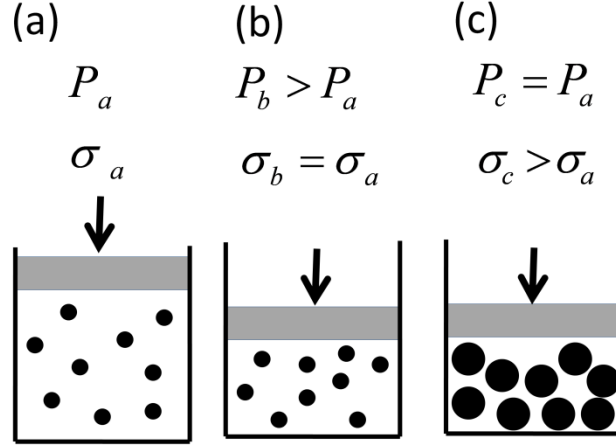


FIG. 8 (a) A liquid is modeled as an ensemble of hard spheres that is subjected to an effective pressure due to particle attractions, P_{eff} . This is schematically shown by hard spheres of size σ_a in a piston in which the applied pressure is P_a . At constant temperature, the volume fraction, ϕ , of the hard spheres can be increased by two distinct mechanisms: by (b) increasing the applied pressure from P_a to P_b , or by (c) increasing the size from σ_a to σ_c , thereby causing the entropic stress, $k_B T / \sigma^3$, to decrease. The mechanism shown in (c) plays the dominate role as σ increases for $\sigma > \sigma_M$ nm at STP. In this range, the decrease in $k_B T / \sigma^3$, overwhelms the decrease in the effective pressure due to attractions, and causes ϕ to increase.

The fact that ϕ increases even as P_{eff} decreases indicates that the change in entropic stress, $k_B T / \sigma^3$, is the dominant mechanism responsible for the σ -induced increase in ϕ . This suggests that it may be possible to approximate the σ -induced increase in ϕ by neglecting the σ -dependence of P_{eff} . We test this by setting $P_{eff} = \bar{P}_{eff}$ for all σ , where $\bar{P}_{eff} = 0.25$ GPa is obtained by averaging values of P_{eff} over the range of $\sigma_1 = 0.42$ nm to $\sigma_g = 0.86$ nm. Values of ϕ calculated using this simplified approach are close to those obtained with the generalized equation of state, as shown by the solid line in FIG. 6. This approximation fails at low ϕ , near the critical point, where values of P_{eff} change significantly with σ_0 . Nevertheless, because the glass transition occurs at elevated values of ϕ , we expect that the effect of P_{eff} on T_g can be approximated by replacing it with a function, \bar{P}_{eff} , that is independent of σ_0 and depends only on temperature.

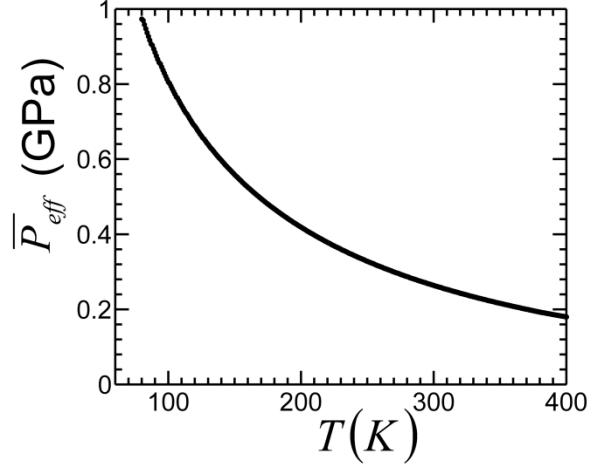


FIG. 9 Dependence of \bar{P}_{eff} on T . Values of \bar{P}_{eff} are obtained by averaging over a range of σ_0 . As T is lowered, both the attractions and the density of particles increase, causing effective pressure of the generalized van der Waal material to increase.

We test this hypothesis by first calculating values of \bar{P}_{eff} for T in range of 60 to 400 K by averaging values of P_{eff} from $\sigma_0 = 0.5$ nm to $\sigma_g(T)$ at each temperature. Values of $\sigma_g(T)$ are calculated from the linear empirical relation shown in Table 2. Calculated values of \bar{P}_{eff} increase as the temperature decreases, as shown in FIG. 9.

The function $\bar{P}_{eff}(T)$ allows us to develop a simplified equation of state in which the effective pressure due to the van der Waals term is replaced with a constant value, \bar{P}_{eff} , that depends only on the temperature, and not on σ_0 . Calculations of the lines of constant ϕ obtained with this simplified approach approximately agree with those obtained with the generalized CS-vdW model, as shown by the solid lines in FIG. 10. Deviations from the generalized CS-vdW occur at elevated values of σ_0 because values of P_{eff} obtained for $\sigma_0 > \sigma_g$ were not averaged to obtain \bar{P}_{eff} . We use this simplified equation of state, together with the function $\phi_g(\sigma_0)$ to predict a glass transition line, $T_g(\sigma_0)$ that agrees well with the experimental data from which $\phi_g(\sigma_0)$ was obtained, as shown by the dashed line in FIG. 10. From this we conclude that the approximate equation of state is in reasonable agreement with the generalized equation of state, in which P_{eff} is allowed to vary with σ_0 . Although using the approximate equation of state is not necessarily practical, it does offer some physical insight into the mechanisms governing the σ_0 -dependence of ϕ . It shows that entropic effects dominate the σ -induced increase in ϕ because the effective pressure due to the generalized van der Waals material does not vary significantly with σ_0 .

Nevertheless the dependence of P_{eff} on T is significant. As temperature decreases at constant P , the system loses thermal energy and compacts. The higher density of particles causes the \bar{P}_{eff} to increase. This dependence is described with the function $\bar{P}_{eff}(T)$, which is useful for describing a “material” relationship that is independent of the particular species, and its size.

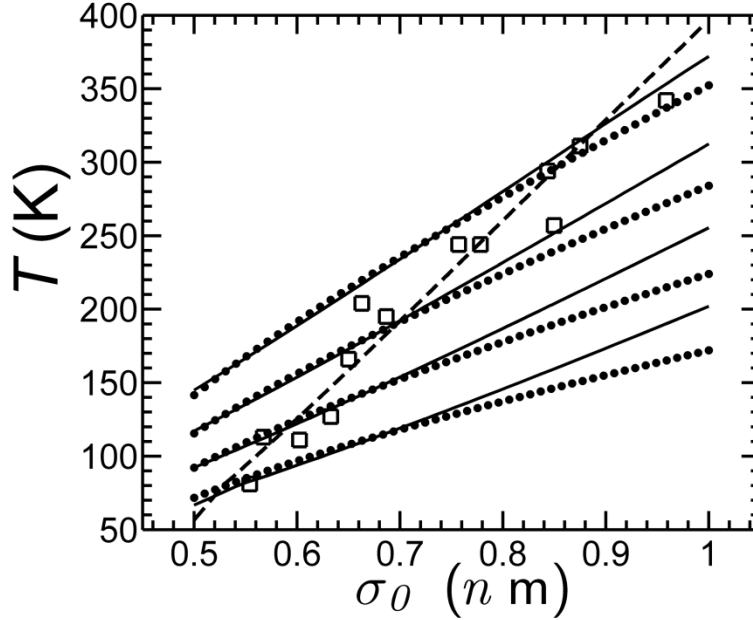


FIG. 10 A simplified model predicts lines of constant ϕ that are similar to those obtained using the generalized equation of state model (shown by the dotted lines, as in FIG. 4). In this approximation, shown by the solid lines, P_{eff} is replaced by a σ_0 -independent function, \bar{P}_{eff} , that depends only on T , and is shown in FIG. 9. Values of ϕ corresponding to each line are shown to the right of the plot. Experimental values of σ_0 and T_g are shown by the open squares and listed in Table 1. The dashed lines show the prediction of $T_g(\sigma_0)$ from the simplified model in which $\bar{P}_{eff}(T)$ and $\phi_g(\sigma_0)$.

V. CONCLUSIONS

We have used tabulated data to generate an generalized equation of state that is a function only of the molecular diameter, σ_0 . The equation is used with an empirical relation for $T_g(\sigma_0)$ to predict how ϕ_g depends on σ_0 for globular, nonpolar molecules, resulting in a model of the σ -induced glass transition that occurs at fixed temperature and pressure. At STP, when $\sigma_g \approx 0.9$

nm, $\phi = \phi_g$ and our model predicts molecules experiencing van der Waals attractions will form a glass. Particles greater than σ_g cannot form a liquid unless steps are taken to reduce the magnitude of the effective attractions, such as dispersing the particles in a solvent as a solute or colloidal phase. We have also shown that the σ -induced increase in ϕ is dominated by entropic effects, and that the effective pressure due to attractions is approximately independent of σ . This observation was used to develop an approximate equation of state in which the size-independent effective pressure, depends only on temperature. This relation, together with $\phi_g(\sigma_0)$ is sufficient to model the dependence of T_g on σ_0 .

A key component of the generalized equation of state is the dependence of τ on σ . This was obtained empirically by fitting results from the literature values obtained from a variety of non-polar molecules. A theoretical understanding of this relationship would require knowledge about how the van der Waals forces that originate from the individual atoms are summed over the volume of the molecule. This integration was performed by Hamaker; [15] the resulting potential applies to molecules that are greater than 0.5 nm in diameter and to colloidal particles. [13] The magnitude of the integral determines the Hamaker constant, which is approximately independent of the size of the molecule, or particle, and does not vary by more than an order of magnitude over a broad range of materials. [13] We expect that by characterizing the empirical relations determined here in terms of the Hamaker constant and the Hamaker pair potential, it will be possible to facilitate additional connections between molecular and colloidal systems.

Acknowledgments

The authors thank Kenneth Schweizer and Johan Mattsson for helpful discussions. This work was performed under Award No. DEFG02-91-ER45439 from the U.S. Department of Energy, University of Illinois at Urbana-Champaign.

References

- [1] C. A. Angell, K. L. Ngai, G. B. McKenna, P.F. McMillan, and S.W. Martin, *J. Appl. Phys.* **88**, 3113 (2000).
- [2] E. R. Weeks, J. C. Crocker, A. C. Levitt, A. Schofield, and D. A. Weitz, *Science*, **287**, 627 (2000).
- [3] P. N. Pusey and W. van Megen, *Nature* **320**, 340 (1986).
- [4] D. Chandler, J. D. Weeks, and H. C. Andersen, *Science* **220**, 787 (1983).
- [5] S. Ramakrishnan and C. F. Zukoski, *J. Chem. Phys.*, **113**, 1237 (2000).
- [6] M. de Loos, B. L. Feringa, and J. H. van Esch, *Eur. J. Org. Chem.*, 3615 (2005).
- [7] M. H. J. Hagen, E. J. Meijer, G. C. A. M. Mooij, D. Frenkel, and H.N.W. Lekkerkerker, *Nature* **365**, 425 (1993).
- [8] F. Cardinaux, T. Gibaud, A. Stradner, and P. Schurtenberger, *Phys. Rev. Lett.* **99**, 118301 (2007).

- [9] M. E. Mackay, T. T. Dao, A. Tuteja, D.L. Ho, B. Van Horn, H.C. Kim, and C.J. Hawker, *Nat. Mater.* **2**, 762 (2003).
- [10] G. Brambilla, D. El Masri, M. Pierno, L. Berthier, L. Cipelletti, G. Petekidis, and A.B. Schofield, *Phys. Rev. Lett.* **102**, 085703 (2009).
- [11] E. Zaccarelli, *J. Phys.-Condens. Mat.* **19**, 323101 (2007).
- [12] W. Gotze, and T. Voigtmann, *Phys. Rev. E* **67**, 021502 (2003).
- [13] J. Israelachvili, *Intermolecular and Surface Forces* (Academic Press, San Diego, California, 1992).
- [14] D. Ben-Amotz and D. R. Herschbach, *J. Phys. Chem.* **94**, 1038 (1990).
- [15] H. C. Hamaker, *Physica* **4**, 1058 (1937).
- [16] D. Ben-Amotz and K. G. Willis, *J. Phys. Chem.* **97**, 7736 (1993).
- [17] P. G. Debenedetti, *Metastable Liquids: Concepts and Principles*, (Princeton University Press, Princeton, NJ, 1996).
- [18] V. P. Privalko, *J. Phys. Chem.* **84**, 3307 (1980).
- [19] G. P. Johari and M. Goldstein, *J. Chem. Phys.* **53**, 2372 (1970).
- [20] C. Gainaru, R. Kahlau, E. A. Rossler, and R. Bohmer, *J. Chem. Phys.* **131**, 184510 (2009).
- [21] S. Corezzi, E. Campani, P. A. Rolla, S. Capaccioli, and D. Fioretto, *J. Chem. Phys.* **111**, 9343 (1999).
- [22] F. Stickel, F. Kremer, and E. W. Fischer, *Physica A* **201**, 318 (1993).
- [23] D. J. Plazek and J. H. Magill, *J. Chem. Phys.* **45**, 3038 (1966).
- [24] A. Bondi, *J. Phys. Chem.* **68**, 441 (1964).
- [25] J. T. Edward, *J. Chem. Educ.* **47**, 261 (1970).
- [26] C. A. Angell, *Polymer* **38**, 6261 (1997).
- [27] P. Bandzuch, J. Kristiak, O. Sausa, and J. Zrubcova, *Phys. Rev. B* **61**, 8784 (2000).
- [28] J. D. Ferry, *Viscoelastic properties of polymers* (Wiley, New York, 1980).
- [29] D. Chandler, *Accounts Chem. Res.* **7**, 246 (1974).
- [30] J. Mattsson, H.M. Wyss, A. Fernandez-Nieves, K. Miyazaki, Z. Hu, D.R. Reichman, and D.A. Weitz, *Nature* **462**, 83 (2009).
- [31] F. Sciortino, *Eur. Phys. J. B* **64**, 505 (2008).
- [32] A. Donev, I. Cisse, D. Sachs, E.A. Variano, F.H. Stillinger, R. Connelly, S. Torquato, and P.M. Chaikin, *Science* **303**, 990 (2004).
- [33] G. Yatsenko and K. S. Schweizer, *Phys. Rev. E* **76**, 041506 (2007).
- [34] L. Berthier and G. Tarjus, *Phys. Rev. Lett.* **103**, 170601 (2009).
- [35] U. R. Pedersen, T. B. Schroder, and J. C. Dyre, *Phys. Rev. Lett.* **105**, 157801 (2010).
- [36] P. Agarwal, H. Qi, and L. A. Archer, *Nano. Lett.* **10**, 111 (2010).